

Compact all-optical switches based on photon-induced suppression of mode interference

Longzhi Li (李龙志), Yi Tang (唐奕),

Jianyi Yang (杨建义), Minghua Wang (王明华), and Xiaoqing Jiang (江晓清)

Department of Information and Electronic Engineering, Zhejiang University, Hangzhou 310027

Received June 3, 2005

An optically activated optical switch based on suppression of mode interference (SMI) is presented. The imaging properties of multi-mode interference (MMI) section in the switch with Y-branch can be modified by a controlling light injection. The switch was simulated by finite difference beam propagation method (FD-BPM) and fabricated on GaAlAs/GaAs epitaxial materials. At the wavelength of $1.31\ \mu\text{m}$, the primary experiment showed an extinction ratio of about 8 dB with controlling light power density of $73.5\ \text{W}/\text{mm}^2$.

OCIS codes: 130.3120, 060.1810, 230.7370.

Since optical switches are the key elements in optical communication networks, lots of works have been devoted to waveguide structures and the types of switches in use including mechanical, thermo-optic, electro-optic, and current-injection^[1] switches, etc.. The waveguide structures mainly include Mach-Zehnder interference (MZI)^[2], Y-branch^[3], total internal reflection^[4,5], and multi-mode interference (MMI)^[6]. The MMI switches, especially S-shaped MMI switches^[6], have the advantages of large fabricating tolerance and small size. In recent years, the ultrafast all-optical switches controlled by light pulses have been researched widely and shown attraction for their ultrafast speed^[5,7-9]. For example, since both the electrons and holes are excited in pairs when the controlling light is injected, the velocity of carrier recombination is faster than that in the case of electrical-current injection. The response speed of the photon-induced carrier effect is faster than that of the electrical-current-induced carrier effects^[5,7].

In this paper, we analyze a novel optical switch based on the suppression of mode interference (SMI)^[10,11] induced by vertical photon-injection. The optically activated SMI optical switch has tremendous potentials in all-optical communication networks for its advantages of small size, simple structure, capability to be monolithically integrated into large optical switch arrays, and ultrafast speed^[10,11].

Figure 1 shows the schematic diagram of the optically

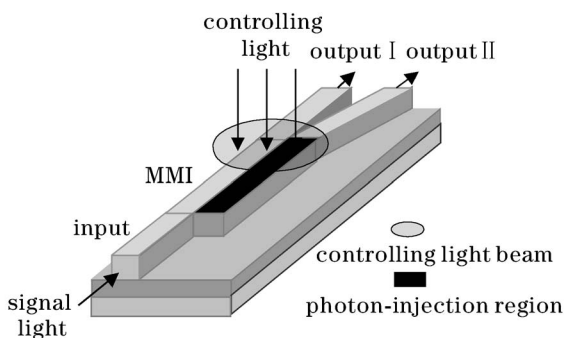


Fig. 1. Schematic diagram of the SMI all-optical switch.

activated SMI optical switch, which consists of a single-mode input channel, MMI, and two single-mode output channels with a branching angle of 3° . The dark long-rectangle area, which is on the right half part of MMI section, is defined as the photon-injection window. The operating principle of SMI all-optical switches is that vertically injecting photons into the MMI section reduces the refractive index of the photon-injection region to change its imaging properties. Without photon-injection, the input light propagates periodically between the left-hand and right-hand of the MMI section, then reaches the output II. The MMI section is several beats long and twice as wide as the input channel.

The switch is simulated by finite difference beam propagation method (FD-BPM), and the result is shown in Fig. 2. From Fig. 2(a), we find that the input light can be converted into output II mostly when the length of MMI is 3 beats in the simulation for transverse electric (TE) mode. When photon-injection is applied, the effect of photon-induced carriers will reduce the refractive index of photon-injection area. For GaAs material, if the density of the injected photons at wavelength of $805\ \text{nm}$ reaches $9.8 \times 10^{11}\ \text{W}/\text{mm}^2$, the change of refractive index Δn at the wavelength of $1.31\ \mu\text{m}$ could reach about -10^{-2} order at $1\text{-}\mu\text{m}$ depth along the injecting direction^[5]. By

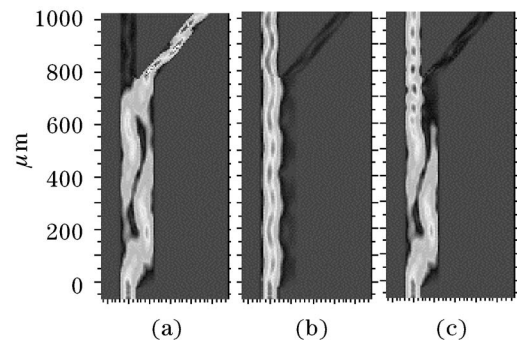


Fig. 2. FD-BPM simulations of SMI all-optical switch in operation. (a) Without photon-injection; (b) with total photon-injection; (c) with partial photon-injection.

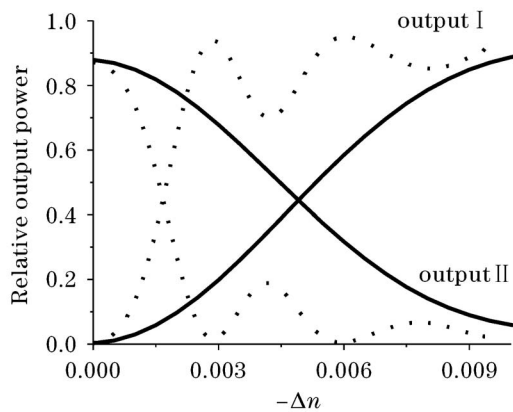


Fig. 3. Relative output power in the output channels I and II versus $-\Delta n$ in the photon-injection region simulated by FD-BPM.

injecting controlling light into the whole photon-injection region, the width of MMI is effectively reduced, then the input light is guided into the output I, as shown in Fig. 2(b). The switch has changed from “off” state to “on” state with 22-dB extinction ratio when Δn in the photon-injection region reaches -0.003 , as illustrated by the dotted curves in Fig. 3. However, if the controlling light is only injected into one part of the photon-injection region, the switching process can be also observed. For example, in our experiment, the diameter of controlling light is $100 \mu\text{m}$, that means the effective length of photon-injection region is also only $100 \mu\text{m}$. If the controlling light beam focuses onto the part of photon-injection region near the output channel branch, the SMI switch has completed the switching process with about 12-dB extinction ratio when Δn reaches -0.01 in the simulation shown in Fig. 2(c), and the output characteristic is described by the solid curves in Fig. 3.

In our experiment, the SMI all-optical switch was fabricated on GaAlAs/GaAs epitaxial materials, which include a $2.5\text{-}\mu\text{m}$ $\text{Al}_{0.07}\text{Ga}_{0.93}\text{As}$ buffer layer and a $1.5\text{-}\mu\text{m}$ GaAs waveguide layer. The rib waveguide was etched by $\text{H}_2\text{PO}_4:\text{H}_2\text{O}_2:\text{H}_2\text{O}$ with the ratio of 1:1:10 and the rib height is $0.9 \mu\text{m}$. The width of the input channel is $6 \mu\text{m}$, while the width and length of MMI section are 12 and $800 \mu\text{m}$, respectively. A 200-nm-thick aluminum layer was deposited on the waveguides and a window was etched as photon-injection region, as shown in Fig. 1.

In the testing system, the controlling light, from an 805-nm laser with the maximum power of 1500 mW, is vertically injected into the photon-injection region, while the signal light is at the 1310-nm wavelength. We collected a series of near-field images of the output channels by changing the density of photon-injection power, as shown in Fig. 4. Figure 5 shows the normalized optical output power versus the photon-injection power density. It is clear that the SMI optical switch has completed the switching process when the photon-injection power density reaches 73.5 W/mm^2 . In this case, the extinction ratio is about 8 dB. To achieve better switching characteristic of SMI, not only the photon-injection power density must be high enough, but also the effective photon-injection region must be large enough. If a cylinder lens is used, the controlling light beam ($\Phi = 100 \mu\text{m}$) can be focused onto the photon-injection region to improve

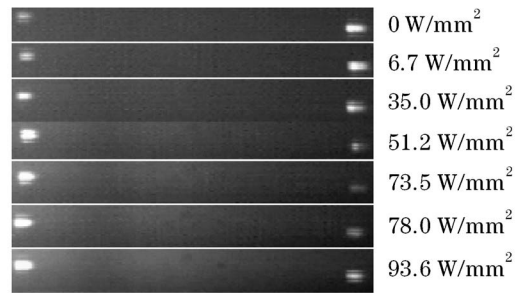


Fig. 4. Near field output of SMI switch with different photon-injection powers.

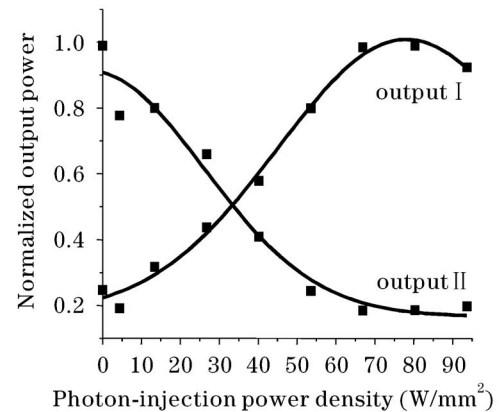


Fig. 5. Normalized optical output power versus photon-injection power density.

the photon-injection power density and lengthen the effective photon-injection region, then higher extinction ratio can be achieved^[5].

In conclusion, we present a compact SMI all-optical switch which modifies the imaging properties of MMI section by injecting a controlling light vertically. The extinction ratio of 8 dB was measured in experiment when the density of the injecting photon was 73.5 W/mm^2 . By improving the efficiency of photon-injection, higher extinction ratio can be achieved. The optically activated SMI optical switches will be attractive components in future all-optical networks for ultrafast speed, simple structure, large scale integration.

This work was supported by the National Natural Science Foundation of China (No. 60177012, 60477018) and the Key Fund of National Natural Science Foundation of China (No. 60436020). X. Jiang is the author to whom the correspondence should be addressed, his e-mail address is iseejxq@zju.edu.cn.

References

1. C. Ciminelli, F. Meli, and G. Grasso, Proc. SPIE **4277**, 33 (2001).
2. Q. Lai, W. Hunziker, and H. Melchior, IEEE Photon. Technol. Lett. **10**, 681 (1998).
3. M. B. J. Diemeer, Opt. Mater. **9**, 192 (1998).
4. J. Yang, Q. Zhou, and R. T. Chen, Appl. Phys. Lett. **81**, 2947 (2002).
5. X. Jiang, J. Yang, H. Zhan, K. Chen, Y. Tang, X. Li, and M. Wang, IEEE Photon. Technol. Lett. **16**, 443 (2004).

6. K.-C. Shu, Y. Lai, and D.-W. Huang, in *Proceeding of OFC'2002* 697 (2002).
7. T. Akiyama, N. Georgiev, T. Mozume, H. Yoshida, A. V. Gopal, and O. Wada, *IEEE Photon. Technol. Lett.* **14**, 495 (2002).
8. M. J. Potasek and T. Campbell, *Proc. SPIE* **4109**, 281 (2000).
9. R. T. Chen, R. Shih, D. Robinson, and T. Jansson, *J. Appl. Phys.* **74**, 5964 (1993).
10. G. A. Fish, L. A. Coldren, and S. P. DenBaars, *Electron. Lett.* **33**, 1898 (1997).
11. G. A. Fish, B. Mason, L. A. Coldren, and S. P. DenBaars, *IEEE Photon. Technol. Lett.* **10**, 1256 (1998).